

Computational Electromagnetic Numerical Code Feature Selected Validation and Verification using Thermal Images of Electromagnetic Fields

John Norgard

NASA/JSC, Houston, TX, USA, Email: john.d.norgard@nasa.gov

Abstract— An infrared (IR) thermal measurement technique is presented to independently validate and verify (V&V) numerical codes used for computational electromagnetic (CEM) field predictions using Feature Selected Validation (FSV) routines . The thermal technique is applied in this paper to V&V new aircraft scattering codes. IR thermal images (temperature distributions) of the electromagnetic (EM) field scattered from a simple, canonical aircraft are measured for selected microwave frequencies, angles-of-incidence, and polarizations. Using a color-temperature table calibrated at NIST/Boulder, the temperature distributions are converted into equivalent field-intensity distributions of the scattered EM field being measured. These IR thermal images (thermograms) are compared to the predicted images (contour plots or relief maps) of the scattered fields calculated with a selected CEM simulation code over the same measurement plane to V&V that the field patterns and the intensity levels are correct. In addition, the measured field can be visualized with the IR thermogram images. A “picture-to-picture” correlation code is used to compare the predicted and measured results and to assess and score their similarities. This is the first step in a progressive approach using a suite of CEM codes to compare predicted results of more sophisticated aircraft geometries with the measured results from the IR thermograms to develop confidence in the complementary measurement and simulation methods.

Keywords—CEM, Coded Validation & Verification, IR Images, FSV

I. INTRODUCTION

An infrared (IR) measurement technique, based on thermal principles, is presented to independently validate and verify (V&V) numerical codes used for computational electromagnetic (CEM) field predictions. The IR technique is applied in this paper to V&V several new aircraft scattering codes, which predict the scattered fields around an aircraft as a function of frequency, angle-of-incidence, and polarization.

In order to gain a better understanding of the electromagnetic (EM) phenomenology associated with complex geometric scattering, a simplified, canonical

scale-model of a typical aircraft (constructed from metallic cylinders, plates, and cones) is considered first, and is tested in an anechoic chamber under limited conditions as an initial step to provide a baseline understanding of the scattering phenomenology.

Later, this study will be extended to compare the experimental measurements and code predictions of EM scattering from more sophisticated hi-fidelity scale models of real conventional aircraft (i.e., F14, F15, F16, etc.), then, later yet, this study will be extended to scale-models of stealthy aircraft (i.e., F22, F34, etc., constructed with composites, radar absorbing materials, meta materials, etc.).

This is the first step in a progressive approach using a suite of CEM codes to compare predicted results of more advanced aircraft geometries and materials with the measured results from the IR thermograms to develop confidence in the complementary measurement and simulation methods.

II. V&V APPROACH

A. Measurements and Models

The IR technique produces a thermal image (temperature distribution) of the scattered EM field over any two-dimensional measurement area (usually a plane) proportional to the intensity of the field being measured. After calibration, this IR thermal image (thermogram) can be compared to the predicted image (2D contour plot or 3D relief map) of the field calculated with a selected CEM scattering code over the same measurement plane to confirm that the experimental measurements and the numerical simulations of the field patterns and the intensity levels agree.

In these comparisons, emphasis is placed on the qualitative similarities and differences (i.e., pattern comparisons), rather than on performing a quantitative evaluation of field intensities in order to identify consistent trends or any anomalies in the results of the IR

and/or computer simulation techniques. This is due partly to the fact that the false color scales are different between the IR/thermal method and the CEM tool used in the simulations making visual comparisons difficult. A “picture-to-picture” correlation code for Feature Selected Validation (FSV) is being developed to compare the measured and predicted images for similarity, and to assess and score their similarities, independent of any differences in the color code used to develop the images.

B. Initial Test Article

As shown in Fig 1, the simple, canonical test article for the initial study consists of a right-cylindrical tube for the fuselage with a conical end cap on the front and a flat end cap on the back. The wings and horizontal stabilizers were constructed from thin, flat, rectangular pieces of metal. The vertical stabilizer was triangular shaped. The scale-model is approximately 50 cm long.

III. MEASUREMENTS

A. Anechoic Chamber Tests

As shown in Fig 2, thermal images of the scattered field from the test article were measured in an anechoic chamber at USAFA, using a horn antenna test setup in conjunction with a novel IR measurement technique.

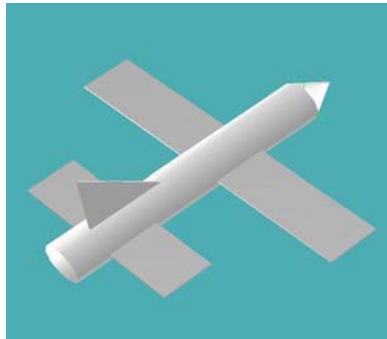


Figure1. Canonical Test Article

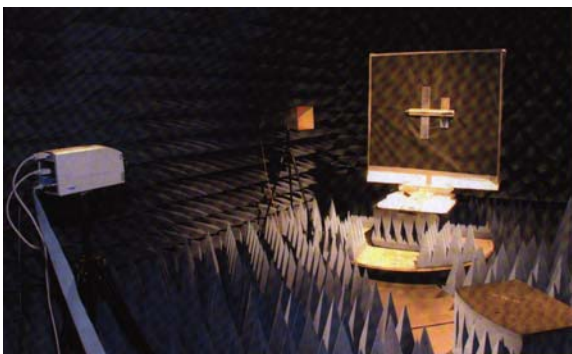


Figure 2. Typical Anechoic Chamber Test Setup Test Article with Horn Antenna and IR camera

B. IR Measurement Technique

The IR measurement technique produces a thermal image (thermogram) of the EM field over a planar two-dimensional area. The temperature distribution in the thermogram is proportional to the intensity of the incident field [1, 2]. After calibration, the images are presented as 2D contour plots or as 3D relief maps of the relative or absolute intensities of the EM fields being measured.

The measured IR thermogram is then compared to the predicted CEM computer simulation of the field (over the same measurement plane) calculated with a numerical CEM code [a hybrid moment method (MoM) and uniform theory of diffraction (UTD) high-frequency ray-tracing code in this case] to confirm the accuracy of the field patterns and intensity levels.

C. IR Detector Screen

The IR measurements are made by placing a thin, lossy (low loss) minimally-perturbing detector screen in the plane over which the field is to be measured. As the wave passes through the screen, some of the EM energy is absorbed by the screen, which, by Joule heating, causes the temperature of the screen to rise over the background ambient temperature of the screen. An IR camera is used to measure the temperature distribution created across the screen. The temperature rise, on a pixel-by-pixel basis, is proportional to the local intensity of the EM field incident on the screen. This is a highly non-linear relationship due to the T^4 temperature dependence for black-body and/or grey-body radiation.

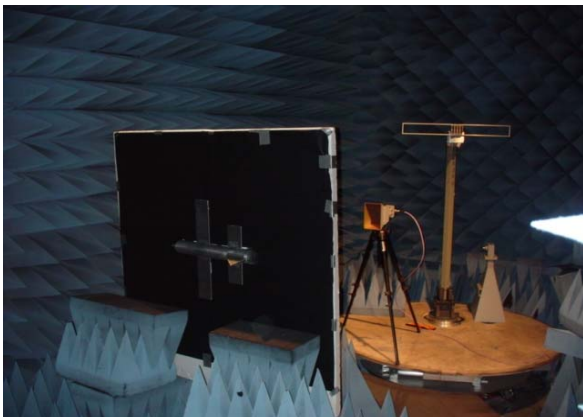
The temperature rise over the ambient background temperature for different screen materials, as a function of the intensity of the field incident on the screen, was measured at NIST/Boulder, and a calibration table of the incident field intensity vs. the color temperature of the screen material was produced. Carbon loaded polyimide films were used in these tests. The color table for a selected screen material (with a specific carbon loading) is used to measure the absolute field intensity of the incident field based on the measured color temperature of the screen.

D. IR Test Setup

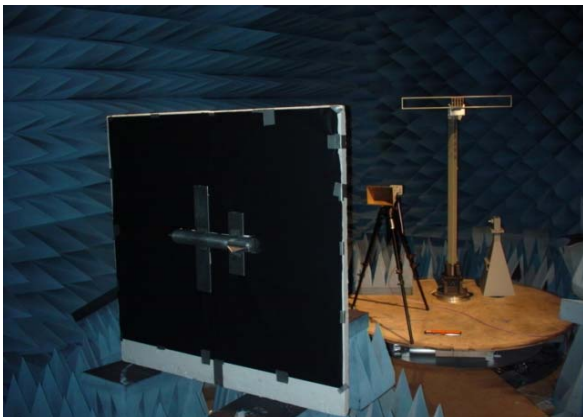
The thin detector screen material was taped onto a flat sheet of Styrofoam. The screen was used to measure the field in the plane of the wings and horizontal stabilizers of the scale-model aircraft, as shown in Fig 3. An outline of the aircraft was cut into the Styrofoam-backed screen material and the model was embedded into screen and taped into position. The screen was positioned just under the wings of the aircraft. The screen with the embedded model was placed inside the anechoic chamber on Styrofoam blocks and irradiated at several selected frequencies in the L, S, and C Bands. The angles-of-incidence were “nose-on”, “tail-on”, “wingtip-on”,

“from-the-top”, and “from-the-bottom”. Two orthogonal polarizations were measured for each angle-of-incidence.

As typical examples of V&V comparisons, the measured thermograms and the corresponding simulated CEM predictions for two polarizations at 3 GHz (10cm) for the “from-the-bottom” angle-of-incidence were selected, where some interesting scattering phenomena were observed both in the measured and simulated models. This is the common case in which the airplane is flying directly overhead and is being irradiated from the ground with two orthogonal polarizations. The experimental test setups are shown in Fig 3; Fig 3a is for axial polarization, and Fig 3b is for transverse polarization (note the rotated horn antenna).



(3a): Axial Polarization



(3b): Transverse Polarization

Figure 3: “From-the-Bottom” Angle-of-Incidence

E. IR Test Results

The scattered fields were measured in the plane of the wings. The thermogram temperature distributions were converted to field intensities (using the color-temperature table calibrated at NIST/Boulder), plotted as false-color images, and compared to similar plots from the selected MoM/UTD numerical code (see Figs 4 and 5). For axial polarization (parallel to the fuselage), the measured thermogram is shown in Fig 4a and the

predicted results in Fig 4b. For transverse polarization (parallel to the wings), the measured thermogram is shown in Fig 5a and the predicted results in Fig 5b.

IV. CEM MODEL

A. Numerical Code Predictions

The CEM model that was used for the simulations mimicked the basic test setup and conditions that were used in the IR measurement technique. The geometrical model was identical in form to the canonical model shown in Fig. 1.

In the initial tests, both a dipole and a horn source were modeled independently in separate runs. For accuracy purposes, the horn antenna required a very detailed description of the source feed and the horn structure at the various frequencies of interest. For simplicity and for the purposes of computational efficiency, and since the initial runs were meant to only verify the generalized scattering patterns from a qualitative viewpoint, the simulations focused on using a far-field dipole as the source instead of the horn antenna model. This provided sufficient results, which could be used to perform the first-order comparisons to the IR measurements. The sampling criterion used in the MoM modeling was 0.1λ where λ is the wavelength at the sample frequency.

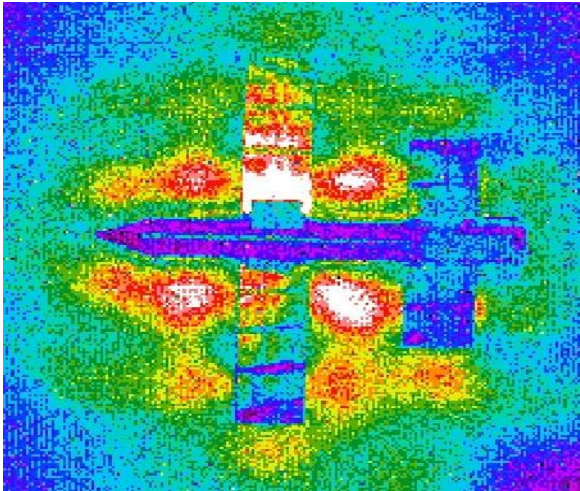
V. V&V TEST OBSERVATIONS

The same essential features of the scattered field are present in both the predicted and the measured images. Note the differences in the color schemes between the measured and the predicted fields, which make the visual comparisons more difficult to correlate and match. Also, the thermal images are saturated in the standing wave areas, so that some of the spherical wave patterns are obscured.

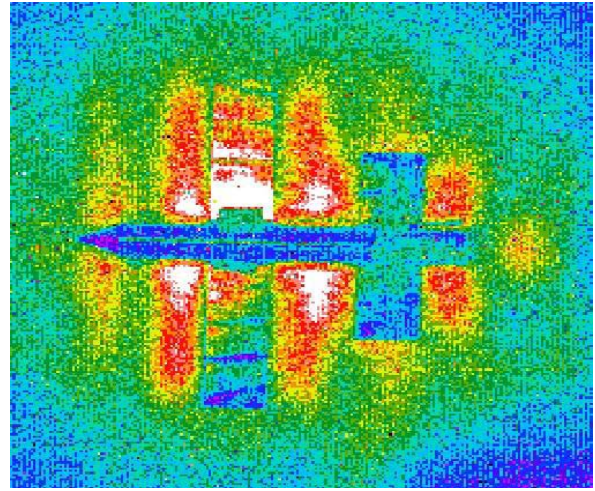
The measured and predicted results of Figs 4 and 5 show good agreement for the spherical standing waves and scattering peaks and nulls around the wings and around the horizontal stabilizers. In addition, the structural resonance and standing wave effects along the cylindrical fuselage can be seen in the figures.

VI. SUMMARY

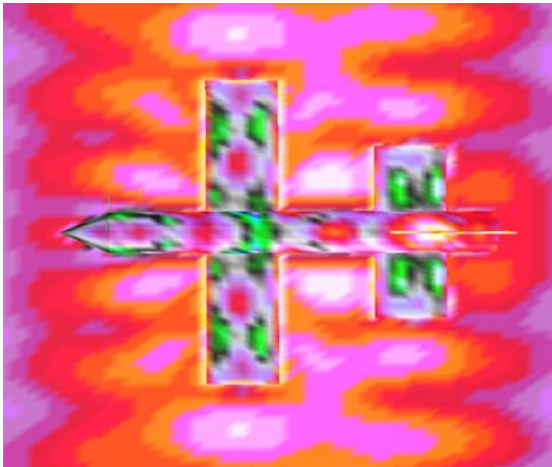
The primary purpose of this study was on applying an IR measurement technique to independently V&V CEM scattering codes using FSV routines. This was done for a simple, canonical, metallic scale-model aircraft. The immediate goal was to determine if two diverse and independent methods of determining the scattered fields could provide similar results relying on a first-level qualitative comparison. The results obtained were found to be in generally good agreement between the IR and computer simulation techniques. Further examination of



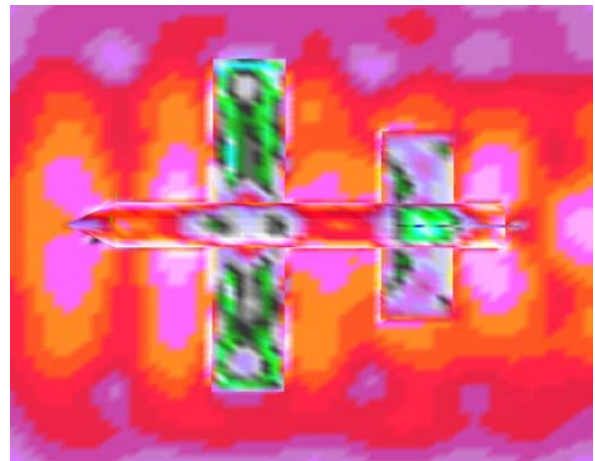
(4a): Measured IR Thermogram



(5a): Measured IR Thermogram



(4b): Simulated CEM Prediction
Figure 4. 3 GHz "From-the-Bottom"
(Axial Polarization)



(5b): Simulated CEM Prediction
Figure 5. 3 GHz "From-the-Bottom"
(Transverse Polarization)

the results of RF measurements of the model at other frequencies, angles-of-incidence, and polarizations, will take place in the future and the approach will be expanded to look at more sophisticated aircraft models.

The results of this study will also be of use to the IEEE EMC Society Standards Development Committee; in particular, it will benefit the IEEE P1597 Working Group charted with the development of standards and recommended practices for validating CEM techniques for EMC applications with routines such as FSV.

REFERENCES

- [1] J. D. Norgard and R. L. Musselman, "Direct IR Measurements of Phased Array Aperture Excitations," QIRT Journal, Vol. 2, No. 1, January 2005, pp.113-126.
- [2] J. D. Norgard and R. L. Musselman, "Direct IR Measurements of Phased Array Near-Field and Far-Field Antenna Patterns," QIRT Journal, Vol. 2, No. 2, July 2005, pp.223-236.